Gas-Phase Nuclear Magnetic Resonance Study of (15N)Trifluoroacetamide: Comparison of Experimental and Computed Kinetic Parameters

Carole L. LeMaster,[†] Clifford B. LeMaster,*,[†] and Nancy S. True[‡]

Contribution from the Department of Chemistry, Boise State University, Boise, Idaho 83725, and Department of Chemistry, University of California, Davis, California 95616

Received May 18, 1998

Abstract: Rate constants obtained from total line-shape analysis of 11 temperature-dependent gas-phase NMR spectra of (15N)trifluoroacetamide yielded the following kinetic parameters: $\Delta G^{\ddagger}_{298} = 15.1(0.36)$ kcal mol^{-1}, $\Delta H^{\ddagger} = 13.3(1.3)$ kcal mol^{-1}, and $\Delta S^{\ddagger} = -5.9(4.5)$ cal mol^{-1} K^{-1}. Ab initio calculations performed at the MP2 level using the 6-311++G(d,p) basis set calculated $\Delta G^{\ddagger}_{298} = 15.19$ kcal mol^{-1}, $\Delta H^{\ddagger} = 14.35$ kcal mol^{-1}, and $\Delta S^{\ddagger} = -2.82$ cal mol^{-1} K^{-1} in reasonable agreement with experiment. Hartree−Fock calculations using that basis set were also in reasonable agreement with experiment, yielding $\Delta G^{\ddagger}_{298} = 16.03$ kcal mol^{-1}, $\Delta H^{\ddagger} = 14.35$ kcal mol^{-1}, and $\Delta S^{\ddagger} = -5.62$ cal mol^{-1} K^{-1}. DFT calculations (B3-PW91) using the same basis set gave results that were considerably less accurate.

Introduction

In this paper we report the first complete gas-phase dynamic NMR study of a primary amide, (15N)trifluoroacetamide ((15N)-TFA). As gas-phase experimental data can be used directly to judge the reliability of theoretical calculations designed to model the C−N torsional potential function and as parametrization data in the development of molecular mechanics and semiempirical molecular orbital calculations, experimental data for primary amides in their isolated state are of significant importance. Unfortunately, gas-phase dynamic NMR studies of primary amides are difficult for several reasons. First, the vapor pressure of primary amides is extremely low, usually less than that for the tertiary amides that have been more extensively studied.[1−11] Vaporization of enough amide for acquisition of gas-phase spectra is further impaired by the affinity of the amide hydrogens for the glass NMR tube. Also, whereas dimethyl amides have three equivalent protons at the exchanging sites, primary amides have only one. Finally, quadrupolar broadening of the hydrogens attached to 14N lowers sensitivity and makes line-shape analysis impossible. The last problem can be solved by substitution of 15N for 14N and the second by hydrophobic treatment of the NMR tube or use of Teflon tubes. Still, our efforts to obtain gas-phase spectra of acetamide have not yet been successful. Substitution of fluorines for hydrogens on the acetamide methyl group increased vapor pressure to a level sufficient to acquire temperature-dependent spectra for line-shape analysis. Berney and Spickerman[12] determined that the vapor pressure of trifluoroacetamide is >1 Torr in the region that exchanging spectra were acquired and at least 0.2 Torr in the region where slow-exchange spectral parameters were obtained.

There has been much recent debate about the origin of the rotational barrier in both amides and thioamides.[13−19] Historically, the amide ground-state resonance structures shown below (**I** and **II**), which give partial double-bond character to the C−N
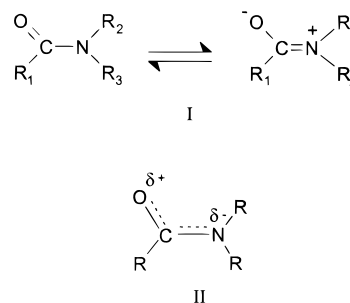

bond, have been used to explain differences in amide rotational barriers upon substitution of various atoms and groups for the hydrogens attached either to the carbonyl carbon or to the amide nitrogen in formamide. More recently, a third resonance structure (**III**) has been added to more completely describe the

† Boise State University.

‡ University of California.

(1) Drakenberg, T. *J. Phys. Chem.* **1976**, *80*, 1023.

(2) (a) Feigel, M. *J. Chem. Soc., Chem. Commun.* **1980**, *10*, 456. (b) Fiegel, M. *J. Phys. Chem.* **1983**, *87*, 3054.

(3) Ross, B. D.; True, N. S.; Decker, D. L. *J. Phys. Chem.* **1983**, *87*, 89.

(4) Ross, B. D.; True, N. S. *J. Am. Chem. Soc.* **1983**, *106*, 2451.

(5) Ross, B. D.; True, N. S.; Matson, G. B. *J. Phys. Chem.* **1984**, *88*, 2675.

(6) LeMaster, C. B.; True, N. S. *J. Phys. Chem.* **1989**, *93*, 1307.

(7) Ross, B. D.; Wong, L. T.; True, N. S. *J. Phys. Chem.* **1985**, *89*, 836.

(8) Suarez, C.; LeMaster, C. B.; LeMaster, C. L.; Tafazzoli, M.; True, N. S. *J. Phys. Chem.* **1990**, *94*, 6697.

(9) Turner, K. A.; LeMaster, C. L.; LeMaster, C. B. *J. Mol. Struct.* **1992**, *271*, 261.

(10) Suarez, C.; Tafazzoli, M.; True, N. S.; Gerrard, S.; LeMaster, C. B.; LeMaster, C. L. *J. Phys. Chem.* **1995**, *99*, 8170.

(11) Neugebauer-Crawford, S. M.; Taha, A. N.; True, N. S.; LeMaster, C. B. *J. Phys. Chem.* **1997**, *101*, 4699.

(12) Berney, C. V.; Spickerman, D. *J. Chem. Thermodyn.* **1978**, *10*, 637.

(13) Wiberg, K. B.; Laidig, K. E. *J. Am. Chem. Soc.* **1987**, *109*, 5935.

(14) Wiberg, K. B.; Breneman, C. M. *J. Am. Chem. Soc.* **1992**, *114*, 831.

(15) Wiberg, K. B.; Rablen, P. R. *J. Am. Chem. Soc.* **1995**, *117*, 2201.

(16) Laidig, K. E.; Cameron, L. M. *J. Am. Chem. Soc.* **1996**, *118*, 1737.

(17) Fogarasi, S.; Szalay, P. G. *J. Phys. Chem. A* **1997**, *101*, 1400.

(18) Glendening, E. D.; Hrabal, J. A., II. *J. Am. Chem. Soc.* **1997**, *119*, 12940.

(19) Lauvergnat, D.; Hiberty, P. C. *J. Am. Chem. Soc.* **1997**, *119*, 9478.

III
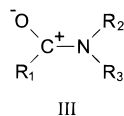
π component of the stabilization of the planar amide structure.[15] For resonance interaction to have a maximum stabilizing effect on the molecule's ground state, planarity of the amide backbone is preferred. Thus, substitution of bulky groups for the formamide hydrogens, which pushes the structure out of its planar configuration, raises the energy of the ground-state molecule. This favors smaller rotational barriers because the 90°-rotated structure (transition state) is now closer in energy to the ground state and the energy required to reach this structure from the ground state is lowered. Because the carbonyl carbon is more electrophilic in the transition state (**IV**) than in the ground state,

IV
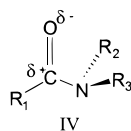
the transition state is more affected by the electronic properties of the R_1 substituent. Using resonance arguments, nucleophilic groups lower the energy of the transition-state structure by stabilizing the electron-deficient carbonyl carbon. This lowers the rotational barrier by placing the transition state closer in energy to the ground state. When electronic and steric effects compete, steric effects usually predominate, indicating that steric destabilization of the ground state (loss of planarity) is more important than electronic effects on the transition-state structure.

Arguments against the resonance model[13,14] are based on observations that the changes in electron distribution and bond lengths that occur during the rotation of formamide do not support electron donation from the amino nitrogen to the carbonyl oxygen as required by the model. Theoretical studies up to the MP2/6-31G(d,p) level calculate the decrease in the length of the C=O bond during rotation to be only about 10% of the increase in length of the C—N bond. These studies also show a higher electron population on nitrogen in the ground-state (planar) structure, which comes at the expense of carbon. The carbonyl oxygen remains virtually unchanged during rotation of the formamide C—N bond. The resonance model would postulate a higher electron population for nitrogen in the rotated transition-state structure, and the decrease in returning to the ground state should come at the expense of oxygen.

Fogarasi and Szalay[17] challenge this argument on two grounds. First, they point out that in conjugated systems the shortening of the single bond is generally about an order of magnitude larger than the lengthening of the double bond. This is partly because the larger force constant of the double bond yields a larger per angstrom energy change. Second, they found, using higher-level calculations (up to CCSD(T)/PVTZ with geometry optimization at that level) than those used by Wiberg et al.[13,14] and Mullikan populations[20] rather than Bader populations,[21] that a charge shift for oxygen was present, that nitrogen shows a negative charge shift upon rotation, and that, although the carbon atom's charge shift fluctuates, the resonance model says nothing about the carbon atom. Thus, the shift of positive charge from nitrogen to oxygen upon amide rotation, predicted by the resonance model, is reproduced by their calculations.

Glendening and Hrabal[18] also attempt to explain the differences in the lengthening of the C—N bond and shortening of the C=O bond. Two electronic effects are considered: conjugative induction between the nitrogen lone pair and the carbonyl π system, which changes the degree of double-bond character of the C=O bond, and hybridization changes, which cause gains and losses of p character. These effects can, in part, account for the difference in the bond length changes. Additionally, their calculations, using the 6-31+G* basis set, with geometries optimized at the RHF, MP2, and B3LYP theory levels, and using natural population analysis and natural resonance theory, show charge density transfer from N to O consistent with the resonance model. This transfer is greater in thioformamide and continues to increase through seleno- and telluroformamide.

Lauvergnat and Hiberty[19] examined the contribution of the delocalization energy to the rotational barrier by calculating the energy difference of the formamide and thioformamide planar ground and rotated states with and without allowing delocalization of nitrogen's lone pair. They found the delocalization energy to be quite significant, contributing about half to the rotational barrier in formamide and two-thirds to thioformamide. Thus, they concluded that resonance is an important contributor to the rotational barrier in formamide and even more important in thioformamide.

This study will compare our theoretical and experimental activation parameters for rotation about the C—N bond in (^{15}N)-TFA. Density functional theory (DFT) has been suggested as an alternative to Møller−Plesset perturbation methods for including electron correlation in such calculations. DFT methods are less costly in computer time. We are interested in the accuracy of this method in predicting amide rotational barriers. This study compares the results of Hartree−Fock (HF), DFT, and MP2 calculations for the prediction of the geometries, energies, and activation parameters of trifluoroacetamide. We will also compare the results of theoretical calculations for trifluoroacetamide with those obtained for formamide[14,17,19] and acetamide.[22]

Experimental Section

NMR Spectroscopy. (^{15}N)Trifluoroacetamide was obtained commercially (MDS Isotopes) and used without further purification. The gas-phase NMR samples were prepared in restricted-volume NMR tubes constructed from 3-cm-long sections of Wilmad high-precision 12-mm coaxial insert tubing. The restricted volume tubes were then inserted into longer 12-mm NMR tubes for introduction into the probe. The short tubes confine the sample and reduce the temperature gradient within the active probe volume. The restricted-volume tubes were evacuated to 30 mTorr before filling. The exchange-region sample consisted of 2 Torr of (^{15}N)TFA, 0.7 Torr of Me_4Si (frequency and resolution reference), and 600 Torr of SF_6 (bath gas, ensures pressures adequate for first-order kinetics). A sample containing 1 Torr of (^{15}N)TFA, 0.7 Torr of Me_4Si, and 300 Torr of SF_6 was used to obtain slow-exchange spectra. The lower (^{15}N)TFA concentration minimizes condensation at the lower temperatures required for acquisition of slow-exchange spectra.

Gas-phase proton NMR spectra were acquired on a wide-bore GE NT-300 spectrometer (proton observation at 300.06 MHz) using a Bradley 12-mm proton probe. Measurements were made on spinning samples in the unlocked mode. The acquisition time was 868 ms per transient with a 0.5-s delay time and a 16-μs pulse width (high power, 98° flip angle). Between 200 and 2000 transients were collected (into 8K memory), depending on the (^{15}N)TFA pressure in the sample and the fine structure in the spectra. Slow-exchange spectra required the most transients. Typical signal-to-noise ratios were 10:1 at slow exchange and 50:1 in the exchange region after multiplication by an

(20) Mulliken, R. S. *J. Chem. Phys.* **1955**, *23*, 1833.

(21) (a) Bader, R. F. W. *Acc. Chem. Res.* **1985**, *18*, 9. (b) Bader, R. F. W. *Atoms in Molecules: A Quantum Theory;* Oxford University Press: Oxford, 1990.

(22) Wong, M. W.; Wiberg, K. B. *J. Phys. Chem.* **1992**, *96*, 668.

exponential line-broadening factor of 5 Hz at slow exchange and 1 Hz in the exchange region. A sweep width of ±2358.49 Hz was used to obtain a digital resolution of 3.47 points/Hz.

Temperatures were controlled with a 0.1° pyrometer and read either before or after each acquisition. Temperature measurements were made using three copper−constantan thermocouples placed within an empty, spinning, 3-cm-long 12-mm-o.d. insert tube placed within an empty 12-mm NMR tube. This arrangement closely resembles the sample system. In this manner the temperature gradient within the active volume of the probe was found to be less than 0.2 K. Samples were allowed to thermally equilibrate at each temperature for at least 10 min prior to initiation of the acquisition.

Rate constants were calculated using the computer program DN-MR5,[23] which uses an iterative nonlinear least-squares regression analysis to obtain the best fit of the experimental NMR spectrum. Exchanging (^{15}N)TFA spectra were analyzed as coupled ABX_3 systems. Slow-exchange spectra indicated that the gas-phase limiting chemical shifts and coupling constants were not temperature-dependent. Slow-exchange proton spectra (obtained between 288.0 and 298.3 K) consisted of a quartet of peaks resulting from chemical shifts of 1632 (5.439 ppm, trans to the carbonyl oxygen) and 1491 Hz (4.969 ppm, cis to the carbonyl oxygen) for the two amino hydrogens with coupling constants, $^1J_{N-H}$, of 90.37 Hz (downfield H, trans to the carbonyl oxygen) and 90.30 Hz (upfield H, cis to the carbonyl oxygen), respectively. These values for chemical shifts and coupling constants were used as input in the line-shape analysis. Coupling constants $^2J_{H-H}$ and $^4J_{F-H}$ were not observed in the gas-phase spectra. They are expected to be very small with $^2J_{H-H} = 1.26$ Hz and $^4J_{F-H} = 1.87$ and ∼0 Hz in DMSO solution.

The effective-line-width parameter was measured at slow and fast exchange. The effective line width was estimated at each temperature by assuming a linear temperature dependence. The line width of Me$_4$-Si was used to estimate the magnetic field inhomogeneity contribution to the line width at each temperature. This factor and the exponential line-broadening factor were added to the interpolated values for the effective line width to obtain the total line broadening and thus the effective transverse relaxation time (T_2) at each temperature where rates were determined. Spectra were analyzed by iterating on the rate constant, spectral origin, baseline height, and baseline tilt. All other parameters were held constant.

Activation parameters were obtained from the rate constants by linear regression of the Eyring equation. A transmission coefficient κ of 0.5 was used in the calculations. Previous studies of amide rotational barriers have used transmission coefficients of either 0.5 or 1.0. For this reason, all data listed and discussed in this paper have been converted to a transmission coefficient of 0.5 for comparison.[24]

Ab Initio Calculations. Ab initio molecular orbital calculations using a 6-311++G(d,p) basis set were performed on a Pentium Pro 200 (dual CPU, Linux operating system) personal computer with 256 MB of memory and a 9 GB hard drive, using the Linux version of Gaussian 94.[25] Minimized structures (fully geometry-optimized), vibrational frequencies for (^{15}N)TFA, and energies of (^{15}N)TFA were calculated for the ground state and two transition states, one having the amino protons staggering the carbonyl oxygen (60° structure) and the other having the amino protons staggering the CCF$_3$ bond (120° structure). (See Figure 1.) For comparison with experimental values, vibrational frequencies were also calculated for the (^{14}N)TFA ground state using

(23) (a) Stephenson, D. S.; Binsch, G. Program No. 365. (b) LeMaster, C. B.; LeMaster, C. L.; True, N. S. Programs No. 569 and QCMP059. Quantum Chemistry Program Exchange, Indiana University, Bloomington, IN 47405.

(24) Note that a decrease in the transmission coefficient from 1.0 to 0.5 increases $\Delta S^{\ddagger}_{298}$ by 1.4 cal K^{-1} mol^{-1} and decreases $\Delta G^{\ddagger}_{298}$ by 0.4 kcal mol^{-1}.

(25) Frisch, M. J.; Trucks, G. W.; Schlegel, H. B.; Gill, P. M. W.; Johnson, B. G.; Robb, M. A.; Cheeseman, J. R.; Keith, T.; Petersson, G. A.; Montgomery, J. A.; Raghavachari, K.; Al-Laham, M. A.; Zakrzewski, V. G.; Ortiz, J. V.; Foresman, J. B.; Peng, C. Y.; Ayala, P. Y.; Chen, W.; Wong, M. W.; Andres, J. L.; Replogle, E. S.; Gomperts, R.; Martin, R. L.; Fox, D. J.; Binkley, J. S.; Defrees, D. J.; Baker, J.; Stewart, J. P.; Head-Gordon, M.; Gonzalez, C.; Pople, J. A., Gaussian 94, Revision D4, Gaussian, Inc., Pittsburgh, PA, 1995.
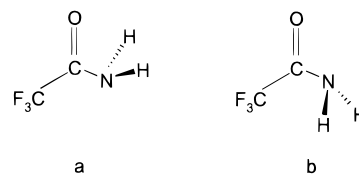

Figure 1. Transition-state structures for trifluoroacetamide: (a) 60° transition state; (b) 120° transition state.

Table 1. Scaling Factors Used for Frequencies in Gaussian Calculations[26]

level of theory	overall	low freq	ZPE	H_{298}	S_{298}
HF/6-311G(d,p)	0.9051	0.9110	0.9248	0.8951	0.9021
B3-PW-91/6-31G(d)	0.9573	0.9930	0.9772	0.9885	0.9920
MP2/6-311G(d,p)	0.9496	1.0127	0.9748	1.0061	1.0175

Table 2. Exchange Rate Constants for (^{15}N)Trifluoroacetamide Gas (Errors Are 2σ)

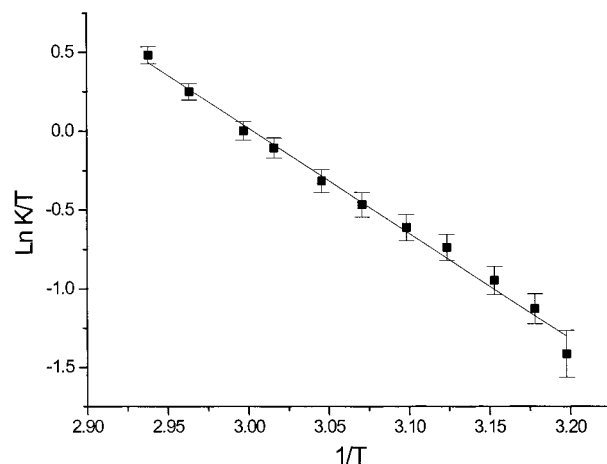| T (±0.1 K)	k (s^{-1})	T (±0.1 K)	k (s^{-1})	T (±0.1 K)	k (s^{-1})
312.8	76(8)	322.8	175(14)	333.7	334(20)
314.7	102(10)	325.7	204(16)	337.5	433(23)
317.2	123(11)	328.4	239(17)	340.4	551(30)
320.2	153(13)	331.6	298(19)		

Figure 2. Eyring plot of the gas-phase exchange rate constants for (^{15}N)trifluoroacetamide.

the optimized geometries. Calculations were performed at the Hartree−Fock, DFT (B3-PW91), and MP2 theory levels.

Frequencies used to obtain the enthalpy, entropy, and free energy of activation at 298 K from the relative energy were scaled according to Scott and Radom[26] and are listed in Table 1 along with the basis sets and theory level for which they were obtained. The scaling-factor values used in the calculations were chosen to best match the basis sets and theory levels used in this study.

Results

Rate constants obtained from total-line-shape analysis of exchange-broadened spectra obtained in the gas phase appear in Table 2, and the Eyring plot generated from those rate constants appears in Figure 2. Selected temperature-dependent gas-phase spectra are shown in Figure 3.

Results of the Gaussian calculations are summarized in Tables 3 and 4, and the MP2 geometries for the ground state of TFA and both transition states are illustrated in Figure 4. Experimentally determined structural data for TFA are not available for comparison. We obtained gas-phase IR spectra of (^{14}N)-TFA (ambient temperature, ∼296 K), which are compared to

(26) Scott, A. P.; Radom, L. *J. Phys. Chem.* **1996**, *100*, 16502.

Table 3. Calculated[a] and Observed Vibrational Frequencies and Intensities for (¹⁴N)Trifluoroacetamide (Calculated Values for (¹⁵N)Trifluoroacetamide Are Given in Parentheses Where Different from Those Calculated for (¹⁵N)Trifluoroacetamide)

MP2 calcd ν (cm⁻¹)[b]	MP2 calcd intens (km mol⁻¹)	DFT calcd ν (cm⁻¹)[c]	DFT calcd intens (km mol⁻¹)	HF calcd ν (cm⁻¹)[d]	HF calcd intens (km mol⁻¹)	obsd ν (cm⁻¹) and intens, gas[e]	obsd ν (cm⁻¹) and intens, soln[f]
29.4	6.0 (5.7)	19.6 (20.3)	6.4 (6.2)	8.4	5.8		
242.3 (241.8)	0.5 (0.7)	239.9 (239.5)	0.7 (0.9)	253.3 (253.0)	0.6		
248.3 (247.0)	8.0 (8.1)	243.4 (242.5)	8.6	255.3 (254.1)	9.4		
330.4 (328.4)	208 (207)	333.6 (330.8)	208	303.4 (301.6)	255.7		295 (w)
373.1 (369.7)	11.1 (11.8)	364.8 (361.1)	4.5 (4.1)	376.5 (372.6)	4.1		
408.7 (408.0)	9.7 (9.3)	403.6 (402.7)	1.4 (1.3)	423.5 (422.6)	1.4		
483.0	1.8	481.9 (481.8)	3.1	504.5	4.2		450 (m)
551.5 (551.3)	8.8	548.3 (548.1)	3.0	564.0 (563.7)	18.5		
557.2 (556.7)	10.7 (10.2)	570.5 (570.2)	10.3 (9.8)	576.6 (576.3)	7.2		580 (vw)
615.6 (611.7)	33.6 (32.7)	614.2 (610.3)	32.1 (30.8)	637.0 (632.7)	44.0		
740.4 (739.6)	7.4 (7.1)	746.7 (745.0)	0.5	780.8 (779.1)	0.4		
750.3 (785.7)	0.9	747.2 (746.5)	11.1 (10.6)	786.4 (785.6)	21.0		
1046 (1037)	6.3 (6.6)	1050 (1041)	8.9 (7.6)	1088 (1078)	8.2 (8.1)		
1122 (1121)	237 (232)	1105	237 (236)	1178 (1175)	279.8	1174 (s)	
1144 (1142)	287 (295)	1143	330	1228 (1227)	418	1200 (s)	1180 (s)
1179 (1177)	349 (352)	1157 (1177)	322 (330)	1238	354	1226 (s)	1210 (s)
1371 (1368)	33.7 (33.9)	1353 (1349)	24.3 (24.4)	1414 (1412)	63.0 (62.8)	1408 (w)	
1552 (1544)	64.7 (62.9)	1550 (1541)	84.6 (81.7)	1609 (1601)	104	1592 (w)	1600 (w)
1729 (1728)	344 (337)	1759 (1757)	401 (395)	1807 (1806)	522	1787 (s)	1750 (s)
3443 (3439)	78.0 (75.3)	3455 (3451)	66.6 (64.1)	3462 (3457)	91.6 (91.7)	3447 (w)	3400 (s)
3576 (3565)	89.2 (88.4)	3582 (3571)	86.0 (85.4)	3587 (3575)	110	3570 (w)	3505 (s)

[a] Scaling factors are from ref 26 (see Table 2). [b] Calculated using a 6-311++G(d,p) basis set for the minimum-energy geometry and scaled by 0.9496. [c] Calculated using a 6-311++G(d,p) basis set for the minimum-energy geometry and scaled by 0.9573. [d] Calculated using a 6-311++G(d,p) basis set for the minimum-energy geometry and scaled by 0.9051. [e] This work. [f] Reference 27.
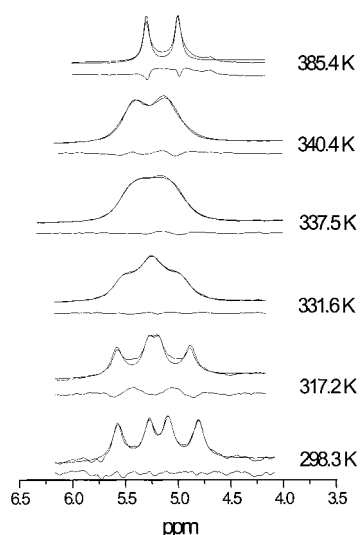

Figure 3. Temperature-dependent gas-phase ¹H NMR spectra of (¹⁵N)-trifluoroacetamide. The sample contained 2 Torr of (¹⁵N)TFA, 0.7 Torr of Me₄Si, and 600 Torr of SF₆. The fitted and experimental spectral lines are overlaid. The lower lines show the difference between the fitted and experimental data.

previously reported condensed-phase values[27] and to the calculated vibrational frequencies in Table 3. Gas-phase IR spectra of TFA are simpler than those obtained in condensed phases where absorptions attributed to dimers and tetramers are observed. For comparison, the calculated harmonic frequencies were scaled using the overall scaling factors listed in Table 1 and agree well with the observed values. Table 4 contains the geometries and energies for the ground state and both transition states and the resulting activation parameters for all three theory levels.

Discussion

The most interesting findings of this study are (1) primary amides exhibit medium effects similar to those of tertiary

amides, (2) the intrinsic (gas-phase) barrier to rotation for trifluoroacetamide is about 1 kcal mol⁻¹ lower than for the *N,N*-dimethyl analogue, (3) MP2 calculations using split-valence basis sets with polarized and diffuse functions are quite accurate for predicting the amino-group rotational activation parameters of (¹⁵N)trifluoroacetamide, but DFT calculations are less accurate than either HF or MP2, and (4) the MP2 calculations for trifluoroacetamide yield a ground-state geometry similar to that obtained for acetamide by Wong and Wiberg.[22] We elaborate on these findings below.

(1) Primary Amides Exhibit Medium Effects Similar to Those of Tertiary Amides. The medium dependence of the rotational barrier in amides has been examined for several tertiary amides and thioamides.[2−11,28,29] Liquid barriers are dependent on solvent and concentration; high polarity and/or amide concentration favor higher amide rotational barriers. Invariably, however, rotational barriers (as measured by $\Delta G^{\ddagger}_{298}$ values) are lower in the gas phase than in the liquid phase, regardless of solvent or concentration. A high-pressure-limit activation energy of 16.6 kcal mol⁻¹ has recently been reported for gaseous [¹⁵N]formamide,[30] but (¹⁵N)TFA is the first primary amide whose rotational barrier has been determined in the gas phase by dynamic NMR methods.

Previously, Ouchi et al.[31] determined the following kinetic parameters ($\kappa = 0.5$) for (¹⁵N)TFA in dioxane (16 mol %) and methyl propyl ketone (18 mol %): $\Delta G^{\ddagger}_{298} = 17.3(0.7)$ kcal mol⁻¹, $\Delta H^{\ddagger} = 17.8(0.8)$ kcal mol⁻¹, and $\Delta S^{\ddagger} = -0.9(2.3)$ cal K⁻¹ mol⁻¹ and $\Delta G^{\ddagger}_{298} = 17.2(0.6)$ kcal mol⁻¹, $\Delta H^{\ddagger} = 17.8(0.8)$ kcal mol⁻¹, and $\Delta S^{\ddagger} = -0.7(0.2)$ cal K⁻¹ mol⁻¹ for the two solvents, respectively. The gas-phase values determined in this study are $\Delta G^{\ddagger}_{298} = 15.1(0.36)$ kcal mol⁻¹, $\Delta H^{\ddagger} = 13.3(1.3)$ kcal mol⁻¹, and $\Delta S^{\ddagger} = -5.9(4.5)$ cal mol⁻¹ K⁻¹. A comparison shows that the activation free energy for amide rotation is about

(27) Troitino, D.; Sanchez de La Blanca, E.; Garcia, M. V. *Spectrochim. Acta* **1990**, *46A*, 1281.

(28) True, N. S.; Suarez, C. *Advances in Molecular Structure Research*; JAI: London, 1995; Vol. I, p 115.

(29) LeMaster, C. B. *Prog. Nucl. Magn. Reson. Spectrosc.* **1997**, *31*, 130−131.

(30) Taha, A. N.; Neugebauer Crawford, S. M.; True, N. S. *J. Am. Chem. Soc.* **1998**, *120*, 1934.

(31) Akiyama, H.; Tachikawa, M.; Furuya, T.; Ouchi, K. *J. Chem. Soc., Perkin Trans. 2* **1973**, 771.

Table 4. Calculated Molecular Parameters for (^{15}N)Trifluoroacetamide[a] (All Methods Used the 6-311++G(d,p) Basis Set)

	GS HF	GS DFT[b]	GS MP2	60° TS HF	60° TS DFT[b]	60° TS MP2	120° TS HF	120° TS DFT[b]	120° TS MP2
r_{CN}	1.3404	1.3490	1.358	1.4147	1.4237	1.4304	1.4122	1.4201	1.4266
r_{CO}	1.1838	1.2064	1.2145	1.1722	1.1942	1.2055	1.1690	1.1907	1.2023
r_{NH} (cis to O)	0.9941	1.0078	1.0092	1.0026	1.0174	1.0183	1.0022	1.0174	1.0181
r_{NH} (trans to O)	0.9915	1.0062	1.0072	1.0026	1.0174	1.0183	1.0022	1.0174	1.0181
r_{CC}	1.5432	1.5530	1.5452	1.5383	1.5507	1.5431	1.5428	1.5571	1.5493
r_{CF}	1.3227	1.3540	1.3515	1.3045	1.3294	1.3299	1.2995	1.3234	1.3237
	1.3081	1.3336	1.3296	1.3147	1.3414	1.3409	1.3201	1.3483	1.3476
	1.3081	1.3336	1.3384	1.3147	1.3414	1.3409	1.3201	1.3483	1.3476
$\angle_{OCN}$	126.2	126.4	126.3	126.9	127.4	127.4	124.7	124.6	124.3
$\angle_{CCN}$	115.1	114.3	114.0	112.6	112.0	111.7	115.7	115.7	115.6
$\angle_{FCC}$	112.1	112.3	112.1	111.6	111.7	111.7	112.6	112.9	112.8
	110.2	110.3	109.8	110.0	110.0	109.9	109.7	109.7	109.6
	110.2	110.3	110.7	110.0	110.0	109.9	109.7	109.7	109.6
$\angle_{CNH}$ (cis to O)	118.1	118.3	117.3	109.5	108.8	108.1	111.2	110.3	109.6
$\angle_{CNH}$ (trans to O)	122.4	122.2	121.1	109.5	108.8	108.1	111.2	110.3	109.6
τ_{OCCF}	180.0	180.0	165.0	0.0	0.0	0.0	0.0	0.0	0.0
	±60.0	±60.0	44.4, −75.5	±120.3	±120.3	±120.3	121.1; −121.0	±121.2	±121.1
τ_{OCNH}	0.0	0.0	−7.6	±58.8	±57.8	±57.4	119.8	±121.1	±121.7
	180.0	180.0	168.8				−119.7		
μ (D)	4.162	4.0872	4.2295	2.7674	2.6617	2.8839	2.901	2.6909	2.9927
vol (cm³ mol⁻¹)	45.21			59.99			63.19		
E (au)	−504.698343	−506.902836	−504.693445	−504.674131	−506.873408	−504.669022	−504.671506	−506.871878	−504.666346
rel E (kcal mol⁻¹)	0	0	0	15.19	18.47	15.32	16.84	19.43	17.00
ZPE[c] (kcal mol⁻¹)	32.17[c]	31.24[d]	31.46[e]	31.69[c]	30.56[d]	30.79[e]	31.62[c]	30.50[d]	30.70[e]
therm corr to E[f] (kcal mol⁻¹)	36.42[g]	35.45[h]	35.57[I]	35.58[g]	34.46[h]	34.60[i]	35.53[g]	34.41[i]	34.53[j]
$\Delta E^{\ddagger}_{298}$ (kcal mol⁻¹)				14.35	17.48	14.35	15.95	18.39	15.96
S (cal K mol⁻¹)	85.18[j]	83.32[k]	81.90[l]	79.56[j]	79.84[k]	79.08[l]	79.90[j]	80.12[k]	79.60[l]
$\Delta S^{\ddagger}_{298}$ (cal K mol⁻¹)				−5.62	−3.48	−2.82	−5.28	−3.20	−2.30
therm corr to H[m] (kcal mol⁻¹)	37.01[g]	36.04[h]	36.16[i]	36.17[g]	35.05[k]	35.19[i]	36.12[g]	35.00[h]	35.12[I]
$\Delta H^{\ddagger}_{298}$ (kcal mol⁻¹)				14.35	17.48	14.35	15.95	18.39	15.96
therm corr to G[n] (kcal mol⁻¹)	11.61	11.20	11.74	12.45	11.25	11.61	12.30	11.11	11.39
$\Delta G^{\ddagger}_{298}$ (kcal mol⁻¹)				16.03	18.52	15.19	17.53	19.34	16.65

[a] Bond lengths are in angstroms, and angles and dihedral angles are in degrees. [b] The B3-PW91 DFT method was used. [c] Frequencies scaled by 0.9248. [d] Frequencies scaled by 0.9772. [e] Frequencies scaled by 0.9748. [f] ZPE + $E(T)$. [g] Frequencies scaled by 0.9248 and 0.8951, respectively. [h] Frequencies scaled by 0.9772 and 0.9885, respectively. [i] Frequencies scaled by 0.9748 and 1.0061, respectively. [j] Frequencies scaled by 0.9021. [k] Frequencies scaled by 0.9920. [l] Frequencies scaled by 1.0175. [m] ZPE + $H(T)$. [n] From S and the thermal correction to H at the appropriate scale factors for each.

2 kcal mol⁻¹ lower in the gas phase than in the liquid phase and that the contribution to $\Delta G^{\ddagger}_{298}$ by the entropy change is greater and that by the enthalpy change is less.

In condensed phases solvent molecule interactions increase the energy required for internal rotation in (^{15}N)TFA. Calculations predict that the transition state is less polar and considerably larger than the ground state. It is possible that solvent molecule interactions lower the energy of the smaller, more polar ground state to a larger extent than the transition state, increasing the relative energy difference from the gas-phase value. Wong and Wiberg[22] predict a nonplanar structure for the acetamide ground state in both the gas (CISD/6-31+G(d,p)) and condensed (self-consistent reaction field HF/6-31+G(d,p), $\epsilon = 40.0$, $a_0 = 3.35$ Å) phases, but the deformation was considerably less in condensed media. The resonance model would postulate that the more planar ground state obtained in condensed media also serves to raise the rotational barrier by increasing the energy difference between the ground and transition states.

Activation entropies for liquid-phase amide rotation in tertiary amides are generally small, but Drakenberg[32] found that $\Delta S^{\ddagger}$ values for rotation of the primary amide acetamide in the solvents *N,N*-dimethylacetamide and acetone were 9 and 5 cal mol⁻¹ K⁻¹, respectively. It was suggested that in primary amides liquid-phase $\Delta S^{\ddagger}$ values are affected by the breaking and forming of amide−proton hydrogen bonds during the rotational process; therefore, liquid-phase $\Delta S^{\ddagger}$ values in primary amides might be expected to be larger than in the gas phase.

(32) Drakenberg, T.; Dahlqvist, K.-I.; Forsén, S. *J. Phys. Chem.* **1972**, *76*, 2178.

(2) The Gas-Phase Barrier to Rotation for Trifluoroacetamide Is About 1 kcal mol⁻¹ Lower Than for the *N,N*-Dimethyl Analogue. Gas- and liquid-phase values of $\Delta G^{\ddagger}_{298}$ for several trifluoroacetamides are listed in Table 5. For the tertiary trifluoroacetamides, the barrier height ($\Delta G^{\ddagger}_{298}$) decreases as the bulk of the amide substituents increases. $\Delta G^{\ddagger}_{298}$ for the primary amide, however, is 0.9 kcal mol⁻¹ lower than for any of the tertiary amides listed. The lower barriers are generally attributed to destabilization of the ground-state structure by the bulky groups, which push the amide backbone away from its preferred planar structure. This increases the ground-state energy by decreasing the resonance-stabilization energy; thus, the additional energy required to reach the transition state is less. Hydrogen atoms are considerably less bulky than any of the tertiary amide constituents, and little, if any, sterically caused out-of-plane deformation would be expected in the primary parent, yet the barrier to rotation of the primary (^{15}N)TFA is lower than that of any of the tertiary trifluoroacetamides listed in Table 5. Moreover, ab initio calculations (at the MP2 level) predict considerable out-of-plane deformation for both acetamide[22] and trifluoroacetamide. For acetamide, this deformation has been attributed to the molecule seeking a conformation in which there is a favorable interaction between the methyl hydrogen and the nitrogen lone pair.[22] Presumably, this would apply as well to the trifluoromethyl fluorine atoms.

(3) Comparison of Experimental and Theoretical Results. Theoretical calculations of $\Delta G^{\ddagger}_{298}$ at the MP2/6-311++G(d,p) level for (^{15}N)trifluoroacetamide are within experimental error of the value obtained from the dynamic NMR study. The calculated activation entropy is also within experimental error.
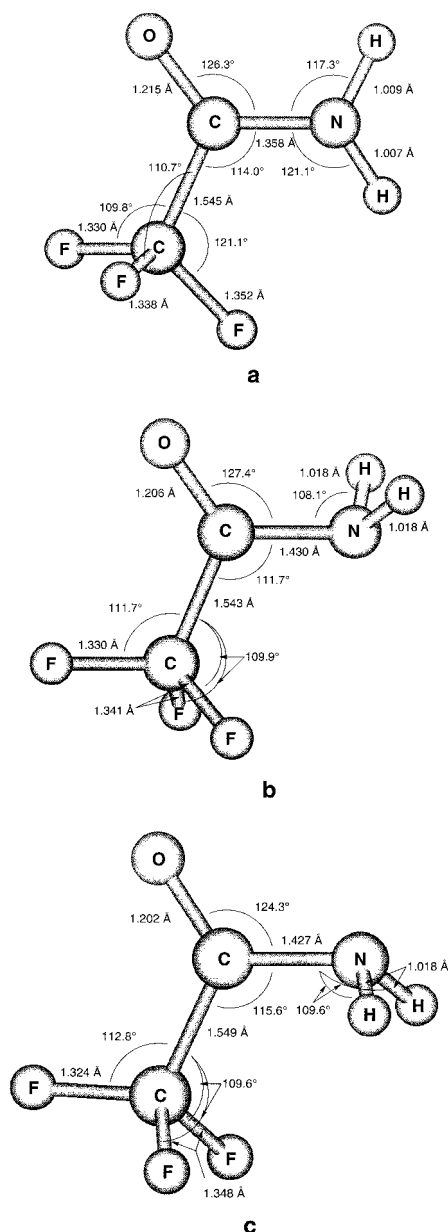
Figure 4. Computed geometries (MP2/6-311++G(d,p)) for trifluoroacetamide: (a) ground state; (b) 60° transition state; (c) 120° transition state.

Table 5. Activation Free Energies for Trifluoroacetamides (CF$_3$COR$_2$) ($\kappa = 0.5$)

		$\Delta G^{\ddagger}_{298}$ (kcal mol^{-1})			
R$_1$	R$_2$	gas	liquid	solvent (mol %)	ref
H	H	15.1 (0.4)	17.3 (0.7)	dioxane (16)	31
CH$_3$	CH$_3$	16.0 (0.5)	17.4 (0.4)	CCl$_4$ (10)	3
CH$_3$	CH$_2$CH$_3$	16.0 (0.1)	17.8 (0.1)	CCl$_4$ (1)	10
CH$_2$CH$_3$	CH$_2$CH$_3$	15.7 (0.1)	17.4 (0.1)	CCl$_4$ (1)	8
isopropyl	isopropyl	15.4 (0.1)	15.9 (0.1)	CCl$_4$ (1)	8
isobutyl	isobutyl	16.0 (0.1)	16.9 (0.1)	CCl$_4$ (1)	8

DFT calculations give a barrier height considerably higher than experiment and less accurate than either HF or MP2 calculations.

Wiberg[33,34] has suggested that the vibrational frequency attributed to the NR$_2$ wag is quite anharmonic and not well-represented by the harmonic treatment afforded in theoretical

(33) Wiberg, K. B.; Rablen, P. R.; Rush, D. J.; Keith, T. A. *J. Am. Chem. Soc.* **1995**, *117*, 4261.

(34) Rush, D. J.; Wiberg, K. B. *J. Phys. Chem. A* **1997**, *101*, 3143.

calculations. In fact, for calculations in acetamide, anharmonic treatment of the NH$_2$ wag increases the ground-state entropy at 298 K by about 1.4 cal mol^{-1} K^{-1}.[35] Furthermore, this same study[35] demonstrates that the methyl rotation, as well, contributes greater entropy to the ground than to the transition state for acetamide (a difference of ∼0.7 cal mol^{-1} K^{-1}). Both these factors lowered the theoretically calculated $\Delta S^{\ddagger}$ value for acetamide, bringing it closer to the experimental value.

We have calculated the change in entropy when the trifluoromethyl rotation in TFA is treated as an internal rotation rather than a low-frequency harmonic vibration. Energies of the ground state and for the 60° and 120° transition states were calculated at 30° increments of the trifluoromethyl group torsional angle using Gaussian 94 (HF/6-311++G**). The calculated 3-fold internal rotation potential functions have barriers of 172, 1028, and 773 cm^{-1} for the ground state and 60° and 120° transition states, respectively. The internal rotation constant, calculated from the ab initio geometry that appears in Table 4, is 0.587 cm^{-1} for the ground state and 0.570 and 0.568 cm^{-1} for the 60° and 120° transition states, respectively.[36] Torsional energy levels were calculated up to an energy of 3000 cm^{-1} for each structure,[37] yielding torsional partition functions of 22.38 for the ground state and 10.78 and 12.40 for the 60° and 120° transition states, respectively, at 298 K. The contributions to $\Delta S^{\ddagger}$ from the trifluoromethyl torsion are −1.459 and −1.180 cal mol^{-1} K^{-1} for the 60° and 120° transition states, respectively. This value replaces the contribution to $\Delta S^{\ddagger}$ by the calculated vibration corresponding to the trifluoromethyl rotation; this is the lowest frequency vibration for the ground state and the lowest frequency nonimaginary vibration for the transition states. Table 6 lists the $\Delta S^{\ddagger}$ values obtained when this replacement is made. The correction increases the value of $\Delta S^{\ddagger}$ in each case and brings the calculated values for all three theory levels into closer agreement.

(4) Comparison with Previous Theoretical and Experimental Studies of Acetamide and Formamide. The molecular parameters of (^{15}N)TFA listed in Table 4 can be compared to previous theoretical calculations of acetamide (AA)[22] and formamide (FA).[14,17,19]

Geometries calculated at the MP2 level for TFA agree well with those obtained previously for acetamide. Ab initio molecular orbital calculations[22] using basis sets up to 6-31+G(d,p) with MP2 electron correlation or configuration interaction (singles and doubles) predict that the lowest-energy geometry of the acetamide ground state has one methyl CH bond almost perpendicular to the plane defined by the heavy atoms and a slightly pyramidal amino group. This structure maximizes the favorable interaction between the nitrogen lone pair and the methyl CH bond. Previous[38] split-valence-basis-set calculations at the Hartree−Fock level yielded planar geometries for acetamide with one C−H bond eclipsed to the carbonyl group. Including p polarizations on heavy atoms yielded conformations with some distortion of the methyl group and out-of-planarity of the amino group. Addition of diffuse functions for heavy atoms further distorts the methyl group. Finally, the electron-correlation calculations (MP2 or CISD) had little further effect

(35) Rush, D. J. Ph.D. Dissertation, Yale University, New Haven, CT, 1996.

(36) Polo, S. R. *J. Chem. Phys.* **1959**, *24*, 1133. The computer program CART, written by J. M. Pickett, calculates the internal rotation constant for trial structures.

(37) Lewis, J. D.; Malloy, J. B.; Chao, T. H.; Laane, J. *J. Mol. Struct.* **1972**, *12*, 427.

(38) See ref 1 of Wong, M. W.; Wiberg, K. B. *J. Phys. Chem.* **1992**, *96*, 668.

Table 6. $\Delta S^{\ddagger}$ Correction for the Trifluoromethyl Rotation (The Trifluoromethyl Rotor Contributes -1.459 and -1.180 cal K^{-1} mol^{-1} to $\Delta S^{\ddagger}$ for the 60° and 120° Transition States, Respectively)

	ν GS (cm^{-1})[a]	contribution of ν to S (cal K^{-1} mol^{-1})	ν TS (cm^{-1})[a]	contribution of ν to S (cal K^{-1} mol^{-1})	$\Delta S^{\ddagger}$ using ν (cal K^{-1} mol^{-1})	$\Delta S^{\ddagger}$ using rotor (cal K^{-1} mol^{-1})
HF: 60° TS	8.4	8.364	72.8	4.076	-5.62	-2.53
HF: 120° TS	8.4	8.364	60.1	4.454	-3.48	-2.55
DFT: 60° TS	20.3	6.603	69.8	4.158	-2.82	-2.49
DFT: 120° TS	20.3	6.603	59.7	4.469	-5.28	-2.25
MP2: 60° TS	31.3	5.748	75.7	4.000	-3.20	-2.80
MP2: 120° TS	31.3	5.748	57.3	4.547	-2.30	-2.28

[a] Scaling factors from Table 1.

on the methyl group, but predict a greater out-of-plane deformation of the amino group.

Results of molecular orbital calculations for the transition-state dihedral angles in acetamide have not been reported. Ab initio calculations with the 6-311++G(d,p) basis set at the Hartree–Fock and DFT (B3-PW91) levels predict that the lowest-energy orientation of the CF$_3$ group in TFA has one C–F bond anti to the carbonyl and a planar amino group. (The barrier to internal rotation of the CF$_3$ group was calculated to be 490 cal mol^{-1}.) MP2 calculations, however, show about a 15° distortion of the trifluoromethyl group from its HF and DFT predicted conformation and the amino hydrogens oriented 8° and 11° out of the amide plane. (See Figure 4.)

Previous theoretical studies[14,17,19] predict planar ($\tau_{OCNH} = 0°$) ground-state structures for formamide; however, considerable dependence on basis set and theory level was observed. While electron correlation tends to shift the structure to nonplanarity, use of electron correlation with very large basis sets (with high angular momentum functions) gives planar results. Apparently, the potential function for formamide is very flat in the area around planarity of the amide backbone; therefore, it is energetically inexpensive (<50 cal mol^{-1})[17] for formamide to deviate from and return to the planar structure.

At the 6-31G*/MP2 level,[14] there is a large calculated increase in the length of the formamide C–N bond, 0.082 Å, and a small decrease in the length of the C=O bond, 0.0069 Å, as the molecule rotates to the transition state. These trends are also observed for TFA and were reported for acetamide.[35] The C–N bond in TFA increases by 0.072 Å while the C=O bond decreases by 0.009 Å for the same rotation. These results have been interpreted as evidence for the limited participation of the oxygen atom (thus, invalidity of the resonance model) in the determination of the rotational barrier in amides.[14] If the resonance model were valid, one might expect more equal, but opposite, changes in the C=O and C–N bond lengths. This conclusion has been questioned by Fogarasi and Szalay,[17] however, who account for slightly more than half of the discrepancy by energy changes. Changes of 0.01 Å toward equilibrium structure values in formamide accounted for energy increases of 144 and 58 μhartrees for the C=O and C–N bonds, respectively. Glendening and Hrabal[18] explain the discrepancy by suggesting the influence of two electronic effects on bond lengths, conjugative interactions and hybridization changes, which were discussed in the introduction of this paper.

Table 7. Comparison of Calculated Activation Parameters for Three Primary Amides

	$\Delta H^{\ddagger}{}_{298}$ (kcal mol^{-1})	$\Delta S^{\ddagger}{}_{298}$ (cal K^{-1} mol^{-1})	$\Delta G^{\ddagger}{}_{298}$ (kcal mol^{-1})
[a]FA → 60° TS	16.86	-1.41	16.99
[a]FA → 120° TS	18.89	-1.48	19.04
[a]AA → 60° TS	14.83	-2.33	15.37
[a]AA → 120° TS	18.37	-2.07	18.83
[b]15N-TFA → 60° TS	14.35	-2.82	15.19
[b]15N-TFA → 120° TS	15.96	-2.30	16.65

[a] MP2/6-31+G** theory level; ref 39. [b] MP2/6-311++G** theory level; this work.

An experimental high-pressure-limit activation energy, E_{∞}, of 16.6(0.3) kcal mol^{-1} has recently been reported for [^{15}N]-formamide.[30] The best calculated value for comparison is a barrier without ZPE corrections of 15.8 kcal mol^{-1} computed at the CCSD(T)/PVTZ level by Fogarasi and Szalay.[17] This value was corrected for ZPE using lower level calculations (MBPT(2)/TZ2P and CCSD/TZP). The magnitude of the ZPE correction was found to be sensitive to the calculation method, and a barrier corrected for ZPE of 15.2(0.5) was estimated. This may be compared to the experimental value[30] of the threshold energy, E_{o}, of 16.3 kcal mol^{-1} at 298 K. ($E_{o} = E_{\infty} - RT + \langle E_{v} \rangle - \langle E_{v}^{+} \rangle$), where the last two terms are the average internal energy of the ground and transition states, 0.54 and 0.22 kcal mol^{-1}, respectively. The average internal energies were calculated using the frequencies in Table III of ref 14.)

Calculated activation parameters for formamide and acetamide (MP2/6-31+G**) have been reported by Rush.[39] These calculations include thermodynamic corrections for the anharmonic nitrogen inversion mode and for methyl rotation. Our calculated parameters (MP2/6-311++G(d,p)) for (^{15}N)TFA, which used scaled ab initio frequencies for all vibrations, are quite similar to those calculated for acetamide and formamide (see Table 7). In all three cases the 60° transition state is predicted to have a lower energy than the 120° structure.

(39) Reference 35, p 409.